Inorg. Chem. **1993**, *32*, 3425–3432

Kinetics and Mechanism of Ligand Substitution Reactions of Pentacyanoferrate(II) Complexes with Bridging N-Heterocyclic Dications in Aqueous Media

Daniel A. Foucher, Donal H. Macartney,* Lauren J. Warrack, and John P. Wilson

Department of Chemistry, Queen's University, Kingston, Ontario, Canada K7L 3N6

Received February 2, 1993

Three series of N-heterocyclic dicationic ligands, $[\mathrm{R(CH_2)}_n\mathrm{R}]^{2+}$, $[\mathrm{R}(o\text{-xyl})\mathrm{R}]^{2+}$, and $[\mathrm{R}(p\text{-xyl})\mathrm{R}]^{2+}$, where R = pyrazine (pyz, n = 3–8), 4,4′-bipyridine (bpy, n = 1–8), and *trans*-1,2-bis(4-pyridyl)ethylene (bpe, n = 1–8), have been synthesized by the reaction of the N-heterocycle with the appropriate α,ω-dibromoalkane, α,α'-dibromo-*o*-xylene, or α,α'-dibromo-*p*-xylene. In addition, ligands with R = 3-methyl- and 3-aminopyrazine, in which the free N donor atom is sterically hindered, have been prepared. These ligands react with the aquapentacyanoferrate(II) ion, $[\mathrm{Fe(CN)_5OH_2}]^{3-}$, to form monomeric, $[\mathrm{Fe(CN)_5L}]^{-}$, and bridged dimeric, $[\mathrm{(NC)_5Fe}(\mu\text{-L})\mathrm{Fe(CN)_5}]^{4-}$, complexes in aqueous solution. The rate and activation parameters for the aqua substitution and ligand dissociation reactions of these complexes have been measured and are found to be consistent with dissociative mechanisms of ligand substitution. The dependence of the rate constants for the formation of $[\mathrm{Fe(CN)_5(R(CH_2)}_n\mathrm{R)}]^{-}$ on the polymethylene chain length n decreases in the order R = pyz > bpy > bpe, as the donor nitrogen atom is further removed from the site of the positive charges. Saturation kinetics are observed in the formation reactions with the dicationic ligands, consistent with an ion-pair dissociative mechanism, with $[\mathrm{Fe(CN)_5OH_2}\|\mathrm{L}]^{-}$ ion-pair constants in the range 40–100 $\mathrm{M^{-1}}$. The rate constants for the rate-determining loss of the coordinated aqua ligand decrease from approximately 300 to 90–130 $\mathrm{s^{-1}}$ upon ion-pairing with the dications. The presence of the amino or methyl substituents *ortho* to the nitrogen coordinated to the $[\mathrm{Fe(CN)_5}]^{3-}$ center results in ligand dissociation rate constants which are 10^3 to 10^4 greater than for ligands in which these substituents are in *meta* positions or are absent. Steric strain energies of 17 and 22 kJ $\mathrm{mol^{-1}}$ have been determined for the amino- and methyl-substituted pyrazinium ligands, respectively.

Introduction

The spectroscopic properties and reaction kinetics of substituted pentacyanoferrate(II) complexes have been of continued interest for the past two decades.[1–3] The ligand substitution reactions of the aquapentacyanoferrate(II) ion with a variety of entering ligands L^{n+}, to form substituted $[\mathrm{Fe(CN)_5L}]^{(3-n)-}$ complexes (eq 1), have been shown to follow a dissociative mechanism,[4–9] with a dependency of k_f on the charge of the entering ligand.

$$[\mathrm{Fe(CN)_5OH_2}]^{3-} + \mathrm{L}^{n+} \underset{k_d}{\overset{k_f}{\rightleftharpoons}} [\mathrm{Fe(CN)_5L}]^{(3-n)-} + \mathrm{H_2O} \quad (1)$$

The dependencies of k_f on the nature of the entering ligand have been attributed to the effects of the position(s) of negative and/or positive charge(s) within the ligand with respect to the available donor atom coordination site(s). For a series of amino acid derivatives as entering ligands, Toma *et al.*[7] observed an increase of approximately 30 $\mathrm{M^{-1}\,s^{-1}}$ in the value of k_f with every additional C–C bond (≈1.3 Å) separating the donor atom from the carboxylate group. The rate constants for the reactions of $[\mathrm{Fe(CN)_5OH_2}]^{3-}$ with a series of $[\mathrm{Co(NH_3)_5L}]^{3+}$ complexes (L is a bridging N-heterocycle) also depend on the distance between the free nitrogen site and the Co(III) metal center.[10–15]

In this paper the results of kinetic and spectroscopic studies of the ligand substitution reactions of pentacyanoferrate(II) complexes with three series of N-heterocyclic dicationic ligands in aqueous solution are reported. The parent N-heterocycles used in this study are pyrazine (pyz), aminopyrazine ($\mathrm{NH_2pyz}$), methylpyrazine ($\mathrm{CH_3pyz}$), 4,4′-bipyridine (bpy), and *trans*-1,2-bis(4-pyridyl)ethylene (bpe). These species have been used frequently as bridging ligands in homo- and heterobinuclear metal complexes.[16] The reaction of the appropriate α,ω-dibromoalkane, α,α'-dibromo-*o*-xylene, or α,α'-dibromo-*p*-xylene with an excess of the N-heterocycle in dimethylformamide or acetonitrile yields the bromide salt of the dications $[\mathrm{R(CH_2)}_n\mathrm{R}]^{2+}$, $[\mathrm{R}(o\text{-xyl})\mathrm{R}]^{2+}$, and $[\mathrm{R}(p\text{-xyl})\mathrm{R}]^{2+}$ (Chart I).

The crystal and molecular structure of $[\mathrm{pyz(CH_2)_3pyz}]\mathrm{Br_2}$ has recently been reported.[17] The $[\mathrm{bpy(CH_2)_3bpy}]^{2+}$ ligand has previously been incorporated into a Ru(II) ammine complex, $[\mathrm{Ru(NH_3)_5(bpy(CH_2)_3bpyH)}]\mathrm{I_5{\cdot}H_2O}$.[18] The $[\mathrm{bpy}(p\text{-xyl})\mathrm{bpy}]^{2+}$ and $[\mathrm{bpy}(o\text{-xyl})\mathrm{bpy}]^{2+}$ cations have been employed as precursors to the formation of cyclic tetracationic host molecules for the

---

(1) Macartney, D. H. *Rev. Inorg. Chem.* **1988**, *9*, 101.
(2) Sielucka, B. *Prog. React. Kinet.* **1989**, *15*, 175.
(3) Stochel, G. *Coord. Chem. Rev.* **1992**, *114*, 269.
(4) Toma, H. E.; Malin, J. M. *Inorg. Chem.* **1973**, *12*, 2080.
(5) Toma, H. E.; Martins, J. M.; Giesbrecht, E. *J. Chem. Soc., Dalton Trans.* **1978**, 1610.
(6) Macartney, D. H.; McAuley, A. *J. Chem. Soc., Dalton Trans.* **1981**, 1780.
(7) Toma, H. E.; Batista, A. A.; Gray, H. B. *J. Am. Chem. Soc.* **1982**, *104*, 7509.
(8) Toma, H. E.; Lever, A. B. P. *Inorg. Chem.* **1986**, *25*, 176.
(9) Macartney, D. H.; Warrack, L. J. *Can. J. Chem.* **1989**, *67*, 1774.
(10) Gaswick, D.; Haim, A. *J. Am. Chem. Soc.* **1974**, *96*, 7845.
(11) Oliveira, L. A. A.; Toma, H. E.; Giesbrecht, E. *Inorg. Chim. Acta* **1977**, *22*, 269.
(12) Malin, J. M.; Ryan, D. A.; O'Halloran, T. V. *J. Am. Chem. Soc.* **1978**, *100*, 2097.
(13) Jwo, J.-J.; Gaus, P. L.; Haim, A. *J. Am. Chem. Soc.* **1979**, *101*, 6189.
(14) (a) Szecsy, A. P.; Haim, A. *J. Am. Chem. Soc.* **1981**, *103*, 1679. (b) Szecsy, A. P.; Haim, A. *J. Am. Chem. Soc.* **1982**, *104*, 3063.
(15) Lee, G.-H.; Della Ciana, L.; Haim, A. *J. Am. Chem. Soc.* **1989**, *111*, 2535.
(16) Steel, P. J. *Coord. Chem. Rev.* **1990**, *106*, 227.
(17) Foucher, D. A.; Fortier, S.; Macartney, D. H. *Acta Crystallogr.* **1989**, *C45*, 112.
(18) Attalla, M. I.; Lawrance, G. A.; Summers, L. A. *Transition Met. Chem.* (*Weinheim, Ger.*) **1985**, *10*, 354.

0020-1669/93/1332-3425$04.00/0

Chart I

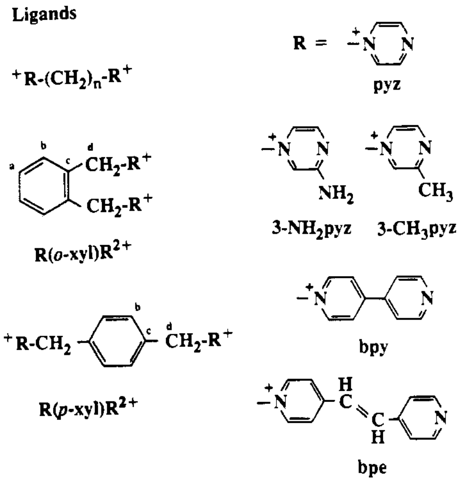

inclusion of amino acids and other organic molecules and for the preparation of novel supramolecular rotaxanes and catenanes.[19]

The rate and activation parameters have been determined for the formation and ligand dissociation reactions (eq 1) of the three series of $[Fe(CN)_5L]^-$ complexes. The dependences of the rate constants on the nature of the N-heterocyclic group and the length of the polymethylene or xylyl linking units are related to the magnitude and distribution of charges on the entering ligand, in terms of an ion-pair dissociative mechanism of ligand substitution. The effects of amino or methyl substituents in a position *ortho* to the nitrogen atom coordinated to the $Fe(CN)_5^{3-}$ center on the rate and activation parameters for the ligand dissociation reactions are investigated.

Experimental Section

Materials. Sodium amminepentacyanoferrate(II) hydrate, $Na_3[Fe(CN)_5NH_3]\cdot 3H_2O$, was prepared by a reported procedure[20] and recrystallized from concentrated ammonia/methanol solutions. Solutions of the aquapentacyanoferrate(II) ion were produced by dissolving the solid ammine complex in nitrogen-saturated distilled water. Low concentrations of the ion ($\leq 5 \times 10^{-5}$ M) were generally used to minimize dimerization. The $[R(CH_2)_nR]^{2+}$ cations were prepared as bromide salts from the reaction of 4,4′-bipyridine, pyrazine, or *trans*-bis-1,2-(4-pyridinyl)ethylene (Aldrich) with the appropriate α,ω-dibromoalkane (Aldrich) in dimethylformamide, by the method reported by Attalla *et al.*,[21] and recrystallized from ethanol/ether mixtures. The yields were in the range 40–80%, generally increasing with the polymethylene chain length. The elemental analyses of the compounds were consistent with the formulas $[pyz(CH_2)_npyz]Br_2$, $[bpy(CH_2)_nbpy]Br_2\cdot xH_2O$ ($x = 0$–3), and $[bpe(CH_2)_nbpe]Br_2\cdot xH_2O$ ($x = 2$–4). Analytical and NMR data (δ) for the lowest member of each series are as follows.

[pyz(CH$_2$)$_3$pyz]Br$_2$. Anal. Calcd for $C_{11}H_{14}N_4Br_2$: C, 36.49; H, 3.83; N, 15.18. Found: C, 36.47; H, 3.84; N, 15.29. ^1H NMR (D_2O): 9.57 (m, H-3), 9.20 (d, H-2, $J_{2,3} = 2.9$ Hz), 5.04 (t, H-α), 2.97 (m, H-β, $J_{\alpha,\beta} = 8.2$ Hz). ^{13}C NMR (D_2O): 151.6 (C-3), 137.6 (C-2, $J(^{14}N-^{13}C) = 8.7$ Hz), 59.2 (C-α), 31.5 (C-β).

[bpy(CH$_2$)bpy]Br$_2$. Anal. Calcd for $C_{21}H_{18}N_4Br_2$: C, 51.94; H, 3.74; N, 11.54. Found: C, 51.72; H, 3.76; N, 11.43. ^1H NMR (D_2O): 9.57 (d, H-2), 8.84 (d, H-2′), 8.74 (d, H-3, $J_{2,3} = 6.8$ Hz), 8.03 (d, H-3′, $J_{2',3'} = 6.0$ Hz), 7.61 (s, H-α). ^{13}C (D_2O): 157.4 (C-4), 150.3 (C-2′), 145.9 (C-2), 141.5 (C-4′), 127.4 (C-3), 122.8 (C-3′), 77.4 (C-α).

[bpe(CH$_2$)bpe]Br$_2$·2H$_2$O. Anal. Calcd for $C_{25}H_{22}N_4Br_2\cdot 2H_2O$: C, 52.34; H, 4.57; N. 9.77. Found: C, 52.12; H, 4.52; N, 9.65. ^1H NMR (DMSO-d_6): 9.60 (d, H-2), 8.73 (d, H-2′), 8.54 (d, H-3, $J_{2,3} = 6.7$ Hz), 8.13 (d, –CH'=), 8.01 (d, –CH–CH=, $J_{H,H'} = 16.5$ Hz), 7.74 (d, H-2, $J_{2,3} = 5.7$ Hz), 7.36 (s, H-α). ^{13}C NMR (DMSO-d_6): 154.8 (C-4), 150.4 (C-2′), 145.5 (C-2), 142.3 (C-4′), 139.8 (–CH'=), 127.8 (–CH=), 125.1 (C-3), 122.1 (C-3′), 75.2 (C-α).

The 1,3-bis(3-aminopyrazinium-1-yl)propane bromide compound was prepared in 45% yield by the reaction of 2-aminopyrzine with 1,3-dibromopropane in dimethylformamide using the method of Attalla *et al.*[21]

[3-NH$_2$pyz(CH$_2$)$_3$3-NH$_2$pyz)]Br$_2$. Anal. Calcd for $C_{11}H_{16}N_6Br_2$: C, 33.75; H, 4.12; N, 21.47. Found: C, 33.33; H, 4.17; N, 21.01. ^1H NMR: 8.56 (d, H-5), 8.06 (d, H-6, $J_{5,6} = 2.8$ Hz), 7.96 (s, H-2), 4.65 (t, H-α), 2.71 (m, H-β, $J_{\alpha,\beta} = 7.7$ Hz). ^{13}C NMR (D_2O): 159.9 (C-3), 149.7 (C-5), 125.4 (C-2, $J(^{14}N-^{13}C = 8.8$ Hz), 123.2 (C-6, $J(^{14}N-^{13}C) = 10.9$ Hz), 58.6 (C-α), 30.9 (C-β).

The xylyl-bridged dications were synthesized in nearly quantitative yields as bromide salts by the reaction of α,α'-dibromo-*o*-xylene or α,α'-dibromo-*p*-xylene (Aldrich) with an excess of the appropriate N-heterocycle in acetonitrile. A solution of 3 mmol of the α,α'-dibromo-xylene dissolved in 15 mL of acetonitrile was added dropwise, over the period of 1 h, to a refluxing solution of 9 mmol of the N-heterocycle in 15 mL of acetonitrile. After gentle refluxing for 3–4 h, the precipitated dibromide salts were filtered out and washed with acetone and ether. The compounds were recrystallized from an ethanol/water mixture and dried under vacuum.

[pyz(*o*-xyl)pyz]Br$_2$. Anal. Calcd for $C_{16}H_{16}N_4Br_2$: C, 45.37; H, 3.81, N, 13.23. Found: C, 45.25; H, 3.89; N, 13.12. ^1H NMR (D_2O): 9.43 (m, H-3), 8.96 (d, H-2, $J_{2,3} = 2.3$ Hz), 7.66 (dd, H-b), 7.44 (dd, H-a, $J_{a,b} = 9.1$ Hz, $J_{a,b'} = 2.1$ Hz), 6.12 (s, H-d). ^{13}C NMR (D_2O): 151.7 (C-3), 137.5 (t, C-2, $J(^{14}N-^{13}C) = 9.0$ Hz), 132.4 and 132.5 (C-a and C-b), 130.1 (C-c), 62.3 (t, C-d, $J(^{14}N-^{13}C) = 3.5$ Hz).

[pyz(*p*-xyl)pyz]Br$_2$. Anal. Calcd for $C_{16}H_{16}N_4Br_2$: C, 45.37, H, 3.81, N, 13.23. Found: C, 45.24; H, 3.83; N, 13.11. ^1H NMR (D_2O): 9.48 (m, H-3), 9.10 (d, H-2, $J_{2,3} = 2.7$ Hz), 7.68 (s, H-b), 6.03 (s, H-d). ^{13}C NMR (D_2O): 153.4 (C-3), 139.4 (t, C-2, $J(^{14}N-^{13}C = 8.9$ Hz), 135.3 (C-b), 133.4 (C-c), 67.2 (C-d).

[bpy(*o*-xyl)bpy]Br$_2$·3H$_2$O. Anal. Calcd for $C_{28}H_{24}N_2Br_2\cdot 3H_2O$: C, 53.40; H, 4.80; N, 8.90. Found: C, 53.58; H, 4.76; N, 8.86.

[bpy(*p*-xyl)bpy]Br$_2$·2H$_2$O. Anal. Calcd for $C_{28}H_{24}N_2Br_2\cdot 2H_2O$: C, 54.97; H, 4.61; N, 9.16. Found: C, 54.92; H, 4.48; N, 9.19.

[bpe(*o*-xyl)bpe]Br$_2$·4H$_2$O. Anal. Calcd for $C_{32}H_{28}N_4Br_2\cdot 4H_2O$: C, 54.92; H, 5.18; N, 8.01. Found: C, 55.39; H, 4.44; N, 8.05.

[py(*o*-xyl)py]Br$_2$·H$_2$O. Anal. Calcd for $C_{18}H_{16}N_2Br_2\cdot H_2O$: C, 49.18; H, 4.59; N, 6.37. Found: C, 49.23; H, 4.58; N, 6.33.

[4-Phpy(*o*-xyl)Phpy]Br$_2$·H$_2$O. Anal. Calcd for $C_{30}H_{26}N_2Br_2\cdot H_2O$: C, 60.89; H, 4.77; N, 4.73. Found: C, 60.58; H, 4.73; N, 4.74.

[3-NH$_2$pyz(*o*-xyl)3-NH$_2$pyz]Br$_2$·H$_2$O. Anal. Calcd for $C_{16}H_{18}N_6Br_2\cdot H_2O$: 39.25; H, 4.53; N, 17.17. Found: C, 39.44; H, 4.46; N, 16.93. ^1H NMR (DMSO-d_6): 8.72 (d, H-5), 8.16 (d, H-6, $J_{5,6} = 3.0$ Hz), 8.10 (s, H-2), 8.06 (s, –NH_2), 7.62 (m, H-b), 7.54 (m, H-a, $J_{a,b} = 9.1$ Hz, $J_{a,b'} = 2.2$ Hz), 6.07 (s, H-d). ^{13}C NMR (D_2O): 158.8 (C-3), 149.8 (C-5), 132.8 (C-a and C-b), 130.3 (C-c), 124.7 (C-2), 123.3 (C-6, $J(^{14}N-^{13}C) = 10.5$ Hz), 61.9 (C-d). The reaction with methylpyrazine yields both the 3-CH_3pyz(*o*-xyl)3-CH_3pyz^{2+} and 2-CH_3pyz(*o*-xyl)3-CH_3pyz^{2+} isomers in a 14:1 ratio (by ^1H NMR), with no evidence for any of the 2-CH_3pyz(*o*-xyl)2-CH_3pyz^{2+} isomer.

[2- and 3-CH$_3$pyz(*o*-xyl)3-CH$_3$pyz]Br$_2$·H$_2$O. Anal. Calcd for $C_{18}H_{20}N_4Br_2\cdot H_2O$: C, 46.04; H, 4.72; N, 11.93. Found: C, 46.10; H. 4.74; N, 11.94.

[2-CH$_3$pyz(*o*-xyl)3-CH$_3$pyz]Br$_2$. ^1H NMR (D_2O, the H-n' resonances refer to the 2-methylpyrazinium half of the molecule): 9.36 (s, H-3), 9.23 (d, H-5), 9.12 (d, H-5′), 8.85 (s, H-2), 8.71 (d, H-6), 8.57 (s, H-6′), 7.63 (m, H-b), 7.52 (m, H-b′), 7.41 (m, H-a), 7.12 (m, H-a′), 6.07 (s, H-d), 6.01 (s, H-d′), 2.92 (s, 2-CH_3), 2.78 (s, CH_3). ^{13}C NMR (DMSO-d_6, the C-$_{n'}$ resonances refer to the 2-methylpyrazinium half of the molecule): 162.8 (C-3), 153.4 (C-3′), 150.8 (C-2), 150.4 (C-5), 148.3 (C-5′), 137.0 (C-2), 136.2 (C-6′), 134.0 (C-6), 132.4 (C-b), 132.2 (C-a), 130.4 (C-b′), 130.3 (C-a′), 130.1 (C-c), 129.3 (C-c′), 62.0 (C-d), 59.0 (C-d′), 22.2 (3-CH_3), 18.3 (2-CH_3).

[3-CH$_3$pyz(*o*-xyl)3-CH$_3$pyz]Br$_2$. ^1H NMR (D_2O): 9.23 (d, H-5), 8.85 (s, H-2), 8.71 (d, H-6), 7.63 (m, H-b), 7.41 (m, H-a), 6.07 (s, H-d), 2.78 (s, CH_3). ^{13}C NMR (DMSO-d_6): 162.8 (C-3), 150.4 (C-5), 137.0 (C-2,

---

(19) (a) Geuder, W.; Hunig, S.; Suchy, A. *Angew. Chem., Int. Ed. Engl.* **1983**, *22*, 489. (b) Anelli, P. L.; Ashton, P. R.; Ballardini, R.; Balzani, V.; Delgado, M.; Gandolfi, M. T.; Goodnow, T. T.; Kaifer, A. E.; Philip, D.; Pietraszkiewicz, M.; Prodi, L.; Reddington, M. V.; Slawin, A. M. Z.; Spencer, N.; Stoddart, J. F.; Vicent, C.; Williams, D. J. *J. Am. Chem. Soc.* **1992,** *114*, 193 and references therein. (c) Goodnow, T. T.; Reddington, M. V.; Stoddart, J. F.; Kaifer, A. E. *J. Am. Chem. Soc.* **1991,** *113*, 4335. (d) Bernardo, A. R.; Stoddart, J. F.; Kaifer, A. E. *J. Am. Chem. Soc.* **1992,** *114*, 10624.

(20) Brauer, G. *Handbook of Preparative Inorganic Chemistry*, 2nd ed.; Academic Press: New York, 1975; Vol. 2, p 1511.

(21) Attalla, M. I.; McAlpine, N. S.; Summers, L. A. *Z. Naturforsch., B* **1984,** *39B*, 74.

Table I. MLCT Band Maxima (nm) and Molar Absorptivity Coefficients for $[Fe(CN)_5L]^{(3-n)-}$ Complexes in Aqueous Solution

	R									
	bpy		bpe		pyz		CH_3pyz		NH_2pyz	
L	λ_{max}	log ε	λ_{max}	log ε	λ_{max}	log ε	λ_{max}	log ε	λ_{max}	log ε
R[a,b]	432	3.75	460	3.86	452	3.70	450	3.71	426	3.64
$[RCH_3]^+$ [a,c]	520	3.75	533	3.84	655	4.08	640	4.02	592	3.65
$[R(CH_2)R]^{2+}$	614	3.84	590	3.85						
$[R(CH_2)_2R]^{2+}$	574	3.82	562	3.84						
$[R(CH_2)_3R]^{2+}$	556	3.81	554	3.86	674	4.22			660	3.90
$[R(CH_2)_4R]^{2+}$	542	3.80	548	3.90	672	4.22				
$[R(CH_2)_5R]^{2+}$	538	3.80	548	3.89	672	4.16				
$[R(CH_2)_6R]^{2+}$	536	3.81	542	3.92	670	4.17				
$[R(CH_2)_7R]^{2+}$	536	3.79	542	3.82	670	4.17				
$[R(CH_2)_8R]^{2+}$	534	3.80	538	3.89	670	4.16				
$[R(o\text{-xyl})R]^{2+}$	598	3.88	560	4.07	692	4.27	680	4.19	604	4.15
$[R(p\text{-xyl})R]^{2+}$	588	3.82			684	4.18				

[a] Reference 4. [b] Reference 13. [c] Reference 9.

$J(^{14}N-^{13}C) = 9.3$ Hz), 134.0 (C-6), 132.4 (C-b), 132.2 (C-a), 130.1 (C-c), 62.0 (C-d), 22.2 (CH_3).

The N-methylated pyrazinium compounds were prepared as iodide salts by the slow addition of an excess of methyl iodide to a refluxing solution of the appropriate substituted pyrazine in CCl_4 or CCl_4/DMF mixture (10:1). The crude products were filtered off and recrystallized from a 4:1 ethanol/water mixture, giving nearly quantitative (>90%) yields. The methylation of 2-methylpyrazine afforded two isomers, 1,2- and 1,3-dimethylpyrazinium iodide, in a 60/40 ratio, which could be distinguished by their needle- and platelike shapes, respectively.

1,2- and 1,3-Dimethylpyrazinium Iodide. Anal. Calcd for $C_6H_9N_2I$: C, 30.53; H, 3.84; N, 11.87. Found: C, 30.56; H, 3.83; N, 11.78.

1,2-Dimethylpyrazinium Iodide. ^1H NMR (D_2O): 9.20 (s, H-3), 9.06 (d, H-6), 8.77 (d, H-5), 4.26 (s, N–CH_3), 2.80 (s, C–CH_3). ^{13}C NMR (D_2O): 152.2 (C-2), 150.8 (C-3), 147.2 (C-5), 135.3 (C-6), 46.8 (N–CH_3), 17.7 (C–CH_3).

1,3-Dimethylpyrazinium Iodide. ^1H NMR (D_2O): 9.16 (d, H-6), 8.81 (d, H-5), 8.68 (s, H-2), 4.35 (s, N–CH_3), 2.73 (s, C–CH_3). ^{13}C NMR (D_2O): 161.9 (C-3), 149.6 (C-5), 138.1 (t, C-2, $J(^{14}N-^{13}C) = 9.4$ Hz), 134.9 (t, C-6, $J(^{14}N-^{13}C) = 9.4$ Hz), 49.2 (t, N–CH_3, $J(^{14}N-^{13}C) = 4.3$ Hz), 21.8 (C–CH_3).

1-Methyl-3-aminopyrazinium Iodide. Anal. Calcd for $C_5H_8N_3I$: C, 25.33; H, 3.41, N, 17.72. Found: C, 25.35; H, 3.40; N, 17.53. ^1H NMR (DMSO-d_6): 8.61 (d, H-5), 8.00 (d, H-6, $J_{5,6} = 3.3$ Hz), 7.98 (s, H-2), 7.82 (s, –NH_2), 4.19 (s, N–CH_3). ^{13}C NMR (D_2O): 158.6 (C-3), 148.8 (C-5), 126.6 (t, C-2, $J(^{14}N-^{13}C) = 9.4$ Hz), 124.2 (t, C-6, $J(^{14}N-^{13}C) = 11.3$ Hz), 48.7 (t, N–CH_3, $J(^{14}N-^{13}C) = 4.3$ Hz).

The methylation of $[bpe(CH_2)_6bpe]^{2+}$ to yield $[bpe(CH_2)_6bpe\text{-}CH_3]IBr_2\cdot 2H_2O$ was achieved by using methyl iodide by the method of Toma.[22] The preparations of $[bpy(CH_2)_6PPh_3]Br_2$ and $[pyz(CH_2)_5py]Br_2$ will be described separately. Solutions of the $[Fe(CN)_5L]^-$ complexes were prepared by adding an excess of the ligand (10^{-3} M) to a nitrogen-saturated solution of aquated $[Fe(CN)_5NH_3]^{3-}$ (10^{-4} M).

Kinetic Measurements. Kinetic measurements were performed by using both stopped-flow and conventional mixing techniques. The kinetics of the slower ligand dissociation reactions were measured on Baush and Lomb Spectronic 2000 and Hewlett-Packard 8452A spectrophotometers with the thermostated cell blocks. The formation reactions and the more rapid ligand dissolution reactions were monitored by using a TDI Model IIA (Cantech Scientific) stopped-flow apparatus and data acquisition system interfaced to a Zenith ZF-151 microcomputer. Pseudo-first-order conditions of excess entering ligand (or excess $[Fe(CN)_5OH_2]^{3-}$ in the studies of the formation of the bridged dimer complexes) were employed, and plots of $\ln(A_\infty - A_t)$ or $\ln(A_t - A_\infty)$ against time were linear for at least 3 half-lives. The first-order rate constants were determined from the average of four to six replicate experiments for the formation reactions and one or two experiments for the ligand dissociation reactions. The reaction temperature was maintained to within 0.1 °C over the range 5–40 °C by means of an external circulating water bath. The ionic strength of the reaction solutions was maintained at 0.10 M with added sodium chloride, and the pH of the solutions was controlled in the pH 6–7 range using phosphate buffers.

Physical Measurements. UV–visible spectra were recorded by using a Hewlett-Packard 8452A diode-array spectrophotometer. The cyclic voltammetric measurements were recorded in aqueous solution with a BAS CV-1B cyclic voltammograph (Bioanalytical Systems) attached to a Houston Instruments 100 X-Y recorder. The working (Pt button) and auxiliary (Pt wire) electrodes in the sample solution were separated from the reference electrode (Ag/AgCl) by a glass frit. The ^1H and ^{13}C NMR spectra were recorded primarily on a Bruker AM-400 instrument, with additional ^1H NMR spectra recorded on a Varian HX-60 instrument. The samples were prepared in D_2O or DMSO-d_6, using added TSP (sodium 3-(trimethylsilyl)propionate) or the residual proton signal from DMSO-d_5, respectively, as an internal reference for the ^1H spectra and external CH_3OH or internal DMSO-d_6 as the chemical shift reference for the ^{13}C spectra.

Results

Electronic Spectra. The addition of an excess of a ligand from the $[R(CH_2)_nR]^{2+}$, $[R(o\text{-xyl})R]^{2+}$, or $[R(p\text{-xyl})R]^{2+}$ series (R = pyz, 3-CH_3, 3-NH_2pyz, bpy, bpe) to an aqueous solution of the $[Fe(CN)_5OH_2]^{3-}$ ion results in aqua ligand substitution and the generation of highly-colored solutions of $[Fe(CN)_5L]^-$ ions (eq 1). The visible spectra of these complexes are dominated by a metal-to-ligand charge-transfer (MLCT) transition (Table I).[4] The positions of the MLCT bands for each series of ligands follow the trend observed with the corresponding N-methylated derivative of the parent N-heterocycle,[9] with a lower energy transition reflecting a greater ability of the ligand to accept electron density from the iron(II) center through π-back-bonding. A dependence of the MLCT energies on the length of the polymethylene chain is found for each of the $[R(CH_2)_nR]^{2+}$ series of the ligands, with the energy increasing with the distance between the positive charges on the ligand. For the longer chains on $[Fe(CN)_5(R(CH_2)_nR)]^-$, $n = 6$–8, the MLCT energy approaches a limiting value, indicating that the second positive charge is no longer felt over this distance. The MLCT energies for the complexes containing the $[R(o\text{-xyl})R]^{2+}$ and $[R(p\text{-xyl})R]^{2+}$ ligands are lower than observed for the corresponding pentacyanoferrate(II) complexes containing $[R(CH_2)_4R]^{2+}$ and $[R(CH_2)_6R]^{2+}$ ligands, respectively, and the complexes with the *o*-xylyl-bridged ligands exhibit slightly lower energy transitions than those containing *p*-xylyl-bridged ligands as the second positive charge is closer and exerts a greater electron-withdrawing effect.

The addition of 2 or more equiv of the $[Fe(CN)_5OH_2]^{3-}$ ion to a solution of the dication ligands results in the formation of a bridged complex $[(NC)_5Fe(\mu\text{-}L)Fe(CN)_5]^{4-}$. There is little change in the MLCT λ_{max} for the bridged complex compared with the monomeric $[Fe(CN)_5L]^-$ species, merely an approximate doubling of the molar absorptivity coefficient.

Electrochemistry. The electrochemistry of the $[Fe(CN)_5L]^-$ complexes was investigated using cyclic voltammetry. The cyclic voltammograms, measured at 25 °C in 0.10 M NaCl (pH 6–7), reveal a quasi-reversible oxidation–reduction process corresponding to the formation of the iron(III) species $Fe(CN)_5L$. The

---

(22) Toma, H. E. *Can. J. Chem.* **1979**, *57*, 2079.

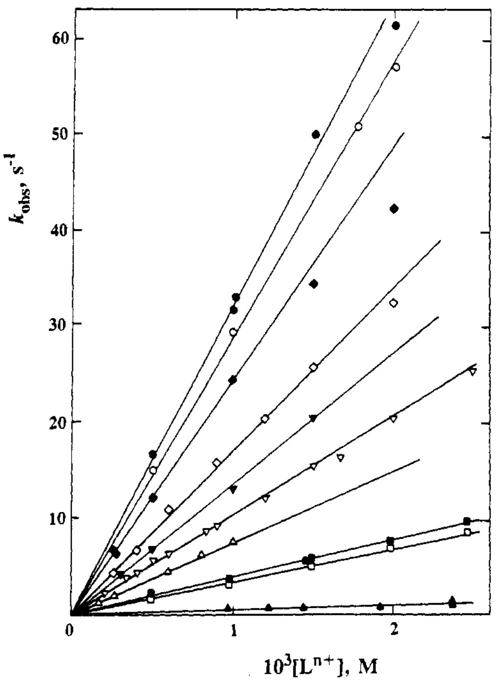

Figure 1. Plots of k_{obs} against $[\mathrm{L}^{n+}]$ for the ligand substitution reactions of the $[\mathrm{Fe(CN)_5OH_2}]^{3-}$ ion with (●) $[\mathrm{3\text{-}NH_2pyz(CH_33\text{-}NH_2pyz}]^{2+}$, (○) $[\mathrm{3\text{-}CH_3pyz(}o\mathrm{\text{-}xyl)3\text{-}CH_3pyz}]^{2+}$, (◆) $[\mathrm{pyz(}o\mathrm{\text{-}xyl)pyz}]^{2+}$, (◇) $[\mathrm{pyz(}p\mathrm{\text{-}xyl)pyz}]^{2+}$, (▼) $[\mathrm{pyz(CH_2)_6pyz}]^{2+}$, (▽) $[\mathrm{bpy(CH_2)_6bpy}]^{2+}$, (△) $[\mathrm{bpe(CH_2)_6bpe}]^{2+}$, (■) $[\mathrm{1\text{-}CH_3\text{-}3\text{-}NH_2pyz}]^{+}$, (□) $[\mathrm{1\text{-}CH_3pyz}]^{+}$, and (▲) $\mathrm{2\text{-}NH_2pyz}$ at 25.0 °C and $I = 0.10$ M.

reduction potentials for the $[\mathrm{Fe(CN)_5L}]^{0/-}$ couples are +0.49 V (vs NHE) for $\mathrm{L}^{2+} = [\mathrm{bpy(CH_2)}_n\mathrm{bpy}]^{2+}$, +0.41 V for $[\mathrm{bpe(CH_2)}_n\mathrm{bpe}]^{2+}$, and +0.78 V for $[\mathrm{pyz(CH_2)}_n\mathrm{pyz}]^{2+}$. These potentials are slightly smaller than the values for the corresponding pentacyanoferrate(II) complexes containing the N-methylated parent heterocycle.[9] The length of the polymethylene bridge has no significant effect on the reduction potential beyond $n = 3$. The reduction potential for the $[\mathrm{Fe(CN)_5(pyz(}o\mathrm{\text{-}xyl)pyz)}]^{0/-}$ couple is +0.83 V. The reduction potentials for the couples containing pyrazinium ligands are also affected by methyl or amino ring substitution, decreasing in both cases. The difference of 20 mV between the potentials of the complexes with 3-methyl-(+0.71 V) and 3-amino-(+0.69 V) substituted 1-methylpyrazinium ligands agrees well with the 26-mV difference reported for the pentacyanoferrate couples where L = 2-methyl- and 2-aminopyridine.[23]

Kinetic Studies. The kinetics of the substitution reactions of the $[\mathrm{Fe(CN)_5OH_2}]^{3-}$ ion with the $[\mathrm{R(CH_2)}_n\mathrm{R}]^{2+}$, $[\mathrm{R(}o\mathrm{\text{-}xyl)R}]^{2+}$, and $[\mathrm{R(}p\mathrm{\text{-}xyl)R}]^{2+}$ dications (L^{2+}) were studied in aqueous solution using stopped-flow techniques. The formations of the monomeric species $[\mathrm{Fe(CN)_5L}]^-$ were studied under pseudo-first-order conditions of excess ligand concentrations and were monitored at their respective visible maxima (Table I). The rate of formation of the substituted $[\mathrm{Fe(CN)_5L}]^-$ complex may be expressed as in eq 2, where $k_{\mathrm{obs}} = k_f[\mathrm{L}^{2+}]$. The observed first-

$$\frac{\mathrm{d}[\mathrm{Fe(CN)_5L^-}]}{\mathrm{d}t} = k_{\mathrm{obs}}[\mathrm{Fe(CN)_5OH_2}^{3-}] \qquad (2)$$

order rate constants displayed a linear dependence on the ligand concentrations ($[\mathrm{L}^{2+}] < 2.5 \times 10^{-3}$ M) for each of the ligands under study (Figure 1). The second-order rate constants and corresponding activation parameters are presented in Table II for R = bpy, Table III for R = bpe, and Table IV for R = pyz, $\mathrm{3\text{-}NH_2pyz}$, and $\mathrm{3\text{-}CH_3pyz}$.

At higher concentrations of the entering ligand ($[\mathrm{L}^{2+}] > 2.5 \times 10^{-3}$ M) curvatures in the dependences of k_{obs} on $[\mathrm{L}^{2+}]$ were observed. Extended concentration ranges of the entering ligand (up to 3.33×10^{-2} M) were investigated for a number of the ligands in this study (Figure 2). The observed dependences of the first-order complexation rate constants on the concentrations of the entering ligand are consistent with an ion-pair dissociative ligand substitution mechanism, as depicted in eqs 3–5. The rate-

$$[\mathrm{Fe(CN)_3OH_2}]^{3-} + \mathrm{L}^{n+} \overset{K_{\mathrm{os}}}{\rightleftharpoons} [\mathrm{Fe(CN)_5OH_2}\|\mathrm{L}]^{(3-n)-} \qquad (3)$$

$$[\mathrm{Fe(CN)_5OH_2}\|\mathrm{L}]^{(3-n)-} \xrightarrow{k_{-\mathrm{w}}} [\mathrm{Fe(CN)_5,L}]^{(3-n)-} + \mathrm{H_2O} \qquad (4)$$

$$[\mathrm{Fe(CN)_5,L}]^{(3-n)-} \xrightarrow{\text{fast}} [\mathrm{Fe(CN)_5L}]^{(3-n)-} \qquad (5)$$

determining loss of the coordinate water molecule is preceded by an outer-sphere ion-pair association, for which K_{os} is dependent on the size and charge of L^{n+1} and on the ionic strength of the reaction medium. With the mechanism in eqs 3–5, the observed first-order rate constants should approach a limiting value of $k_{-\mathrm{w}}$ at sufficiently high concentrations of the entering ligand. A fit of these rate constants to eq 6, where m is the number of ligand

$$k_{\mathrm{obs}} = \frac{mk_{-\mathrm{w}}K_{\mathrm{os}}[\mathrm{L}^{n+}]}{1 + K_{\mathrm{os}}[L^{n+}]} \qquad (6)$$

donor atoms ($m = 2$ for most of the ligands in this study), will yield estimates of $k_{-\mathrm{w}}$ and K_{os}. Least-squares fits of the kinetic data for the curved portions of Figure 2 to a double reciprocal plot of $2/k_{\mathrm{obs}}$ against $1/[\mathrm{L}^{2+}]$ yielded the values of $k_{-\mathrm{w}}$ and K_{os} presented in Table V.

The outer-sphere association constants for ion pairs formed between the $[\mathrm{Fe(CN)_6}]^{4-}$ ion (the $[\mathrm{Fe(CN)_5OH_2}]^{3-}$ ion was not employed due to the dimerization processes which occur at higher concentrations) and the noncoordinating $[\mathrm{R(}o\mathrm{\text{-}xyl)R}]^{2+}$ cations (eq 7), where R is pyridine or 4-phenylpyridine, were determined

$$[\mathrm{Fe(CN)_6}]^{4-} + [\mathrm{R(}o\mathrm{\text{-}xyl)R}]^{2+} \overset{K_{\mathrm{os}}}{\rightleftharpoons} [\mathrm{Fe(CN)_6}\|\mathrm{R(}o\mathrm{\text{-}xyl)R}]^{2-} \qquad (7)$$

by monitoring the outer-sphere charge-transfer band[21] associated with the $[\mathrm{Fe(CN)_6}\|\mathrm{R(}o\mathrm{\text{-}xyl)R}]^{2-}$ species at 25.0 °C and $I = 0.10$ M (NaCl). The $[\mathrm{Fe(CN)_6}\|\mathrm{py(}o\mathrm{\text{-}xyl)py}]^{2-}$ outer-sphere ion pair has a $\lambda_{\max}$ at 394 nm ($\epsilon = 122 \pm 15\ \mathrm{M^{-1}\,cm^{-1}}$), with $K_{\mathrm{os}} = 190 \pm 30\ \mathrm{M^{-1}}$. The $[\mathrm{Fe(CN)_6}\|\mathrm{4\text{-}Phpy(}o\mathrm{\text{-}xyl)4\text{-}Phpy}]^{2-}$ outer-sphere ion pair has a $\lambda_{\max}$ at 444 nm ($\epsilon = 105 \pm 10\ \mathrm{M^{-1}\,cm^{-1}}$), with $K_{\mathrm{os}} = 155 \pm 25\ \mathrm{M^{-1}}$. Toma has determined the outer-sphere ion pair association constants for the interactions of the substitution-inert $[\mathrm{Fe(CN)_6}]^{4-}$ ion with N-heterocyclic cations, such as 1-methylpyrazinium ($K_{\mathrm{os}} = 10\text{–}13\ \mathrm{M^{-1}}$), and dications, such as 1,1′-dimethyl-4,4′-bipyridinium ($K_{\mathrm{os}} = 30\text{–}40\ \mathrm{M^{-1}}$).[21] The higher values for the $[\mathrm{py(}o\mathrm{\text{-}xyl)py}]^{2+}$ and $[\mathrm{4\text{-}Phpy(}o\mathrm{\text{-}xyl)4\text{-}Phpy}]^{2+}$ dications are likely due to the closer proximity of the two positive charges. The K_{os} values for corresponding $[\mathrm{Fe(CN)_5OH_2}\|\mathrm{L}]^-$ ions are expected to be somewhat smaller with the charge of -3 on the $[\mathrm{Fe(CN)_5OH_2}]^{3-}$ ion. The outer-sphere constants determined for the ion pairs with the $[\mathrm{pyz(}o\mathrm{\text{-}xyl)pyz}]^{2+}$ and $[\mathrm{bpy(}o\mathrm{\text{-}xyl)bpy}]^{2+}$ ligands from eq 6 are therefore quite reasonable.

Formation of the Bridged Complexes. The kinetics of the formation of the bridged dimeric species, $[\mathrm{(CN)_5Fe(}\mu\mathrm{\text{-}L)Fe(CN)_5}]^{4-}$, were studied (eq 8) by using a pseudo-first-

$$[\mathrm{Fe(CN)_5OH_2}]^{3-} + [\mathrm{Fe(CN)_5L}]^- \xrightarrow{k_2} [\mathrm{(CN)_5Fe(}\mu\mathrm{\text{-}L)Fe(CN)_5}]^{4-} \qquad (8)$$

---

(23) Brisset, J.-L.; Biquard, M. *Inorg. Chim. Acta* **1981**, *53*, L125.

(24) Malin, J. M.; Brunschwig, B. S.; Brown, G. M.; Kwan, K.-S. *Inorg. Chem.* **1981**, *20*, 1438.

Table II. Rate and Activation Parameters for the Reaction of $[\mathrm{Fe(CN)_5OH_2}]^{3-}$ with $[\mathrm{bpy(CH_2)}_n\mathit{bpy}]^{2+}$ and $[\mathrm{bpy(xyl)bpy}]^{2+}$ and the Ligand Dissociation of $[\mathrm{bpy(CH_2)}_n\mathrm{bpy}]^{2+}$ and $[\mathrm{bpy(xyl)bpy}]^{2+}$ from $[\mathrm{Fe(CN)_5L}]^{(3-n)-}$ in Aqueous Solution[a]

ligand L^{n+}	$10^{-4}k_\mathrm{f}$,[b] $\mathrm{M^{-1}\,s^{-1}}$	$\Delta H_\mathrm{f}^{\ddagger}$, kJ $\mathrm{mol^{-1}}$	$\Delta S_\mathrm{f}^{\ddagger}$, J $\mathrm{K^{-1}\,mol^{-1}}$	10^3k_d,[b] $\mathrm{s^{-1}}$	$\Delta H_\mathrm{d}^{\ddagger}$, kJ $\mathrm{mol^{-1}}$	$\Delta S_\mathrm{d}^{\ddagger}$, J $\mathrm{K^{-1}\,mol^{-1}}$
bpy	0.509 ± 0.002	63.6 ± 2.5	26 ± 8	0.62[c]	111 ± 2[c]	67 ± 6[c]
$[\mathrm{bpyCH_3}]^{+}$ [d]	0.282 ± 0.011	68.2 ± 4.2	50 ± 13	2.64	110 ± 3	76 ± 9
$[\mathrm{bpy(CH_2)bpy}]^{2+}$	1.15 ± 0.04	66.1 ± 1.7	54 ± 5	2.66	107 ± 3	65 ± 9
$[\mathrm{bpy(CH_2)_2bpy}]^{2+}$	1.38 ± 0.07	61.9 ± 2.9	42 ± 9	3.86	102 ± 6	50 ± 18
$[\mathrm{bpy(CH_2)_3bpy}]^{2+}$	1.20 ± 0.09	59.4 ± 1.3	32 ± 4	3.54	98 ± 3	35 ± 9
$[\mathrm{bpy(CH_2)_4bpy}]^{2+}$	1.32 ± 0.09	62.3 ± 2.1	43 ± 6	3.50	99 ± 4	39 ± 12
$[\mathrm{bpy(CH_2)_5bpy}]^{2+}$	1.01 ± 0.03	65.3 ± 1.7	51 ± 5	2.98	102 ± 5	48 ± 16
$[\mathrm{bpy(CH_2)_6bpy}]^{2+}$	1.02 ± 0.03	61.1 ± 0.5	37 ± 2	3.04	101 ± 6	46 ± 19
$[\mathrm{bpy(CH_2)_7bpy}]^{2+}$	0.907 ± 0.015	58.4 ± 1.8	27 ± 5	3.51	105 ± 1	59 ± 4
$[\mathrm{bpy(CH_2)_8bpy}]^{2+}$	0.980 ± 0.030	61.5 ± 1.3	38 ± 4	2.80	103 ± 6	52 ± 18
$[\mathrm{bpy(CH_2)_6PPh_3}]^{2+}$	0.357 ± 0.003	66.5 ± 2.5	46 ± 8	1.72	110 ± 2	71 ± 8
$[\mathrm{bpy(}o\mathrm{\text{-}xyl)bpy}]^{2+}$	1.09 ± 0.10	64.9 ± 1.7	50 ± 5	2.79	102 ± 3	47 ± 7
$[\mathrm{bpy(}p\mathrm{\text{-}xyl)bpy}]^{2+}$	0.993 ± 0.018	61.1 ± 2.9	36 ± 8	2.83	100 ± 6	42 ± 18

[a] At pH 7, $I = 0.10$ M. [b] At 25.0 °C. [c] Reference 4, $I = 0.50$ M. [d] Reference 9.

Table III. Rate and Activation Parameters for the Reaction of $[\mathrm{Fe(CN)_5OH_2}]^{3-}$ with $[\mathrm{bpe(CH_2)}_n\mathrm{bpe}]^{2+}$ and $[\mathrm{bpe(}o\mathrm{\text{-}xyl)bpe}]^{2+}$ and the Ligand Dissociation of $[\mathrm{bpe(CH_2)}_n\mathrm{bpe}]^{2+}$ and $[\mathrm{bpe(}o\mathrm{\text{-}xyl)bpe}]^{2+}$ from $[\mathrm{Fe(CN)_5L}]^{(3-n)-}$ in Aqueous Solution[a]

ligand L^{n+}	$10^{-3}\,k_\mathrm{f}$,[b] $\mathrm{M^{-1}\,s^{-1}}$	$\Delta H_\mathrm{f}^{\ddagger}$, kJ $\mathrm{mol^{-1}}$	$\Delta S_\mathrm{f}^{\ddagger}$, J $\mathrm{K^{-1}\,mol^{-1}}$	$10^3\,k_\mathrm{d}$,[b] $\mathrm{s^{-1}}$	$\Delta H_\mathrm{d}^{\ddagger}$, kJ $\mathrm{mol^{-1}}$	$\Delta S_\mathrm{d}^{\ddagger}$, J $\mathrm{K^{-1}\,mol^{-1}}$
bpe[c]	0.683 ± 0.023	65.3 ± 4.6	28 ± 14	1.12	102 ± 1	41 ± 4
$[\mathrm{bpeCH_3}]^{+}$ [c]	2.71 ± 0.11	59.8 ± 2.5	22 ± 8	2.44	103 ± 1	52 ± 4
$[\mathrm{bpe(CH_2)bpe}]^{2+}$	7.42 ± 0.21	66.1 ± 4.2	51 ± 13	2.56	95 ± 2	26 ± 6
$[\mathrm{bpe(CH_2)_2bpe}]^{2+}$	7.82 ± 0.26	64.4 ± 0.8	45 ± 3	2.55	97 ± 4	29 ± 12
$[\mathrm{bpe(CH_2)_3bpe}]^{2+}$	6.99 ± 0.48	64.0 ± 3.3	44 ± 10	3.04	95 ± 5	26 ± 15
$[\mathrm{bpe(CH_2)_4bpe}]^{2+}$	7.81 ± 0.44	66.5 ± 5.0	53 ± 15	2.70	101 ± 3	46 ± 9
$[\mathrm{bpe(CH_2)_5bpe}]^{2+}$	7.22 ± 0.58	67.8 ± 3.3	44 ± 10	3.12	96 ± 1	31 ± 3
$[\mathrm{bpe(CH_2)_6bpe}]^{2+}$	7.52 ± 0.24	66.1 ± 2.1	52 ± 6	2.72	98 ± 3	35 ± 9
$[\mathrm{bpe(CH_2)_7bpe}]^{2+}$	7.71 ± 0.42	63.6 ± 2.5	43 ± 8	2.03	100 ± 2	38 ± 6
$[\mathrm{bpe(CH_2)_8bpe}]^{2+}$	7.58 ± 0.47	63.6 ± 3.8	42 ± 11	2.27	101 ± 3	44 ± 9
$[\mathrm{bpe(CH_2)_6bpeCH_3}]^{3+}$	7.01 ± 0.17	64.9 ± 3.8	46 ± 11	3.10	89 ± 1	4 ± 3
$[\mathrm{bpe(}o\mathrm{\text{-}xyl)bpe}]^{2+}$	7.55 ± 0.33	63.2 ± 2.1	41 ± 6	5.41	110 ± 2	59 ± 6

[a] At pH 7, $I = 0.10$ M (NaCl). [b] At 25.0 °C. [c] Reference 9.

Table IV. Rate and Activation Parameters for the Reaction of $[\mathrm{Fe(CN)_5OH_2}]^{3-}$ with $[\mathrm{pyz(CH_2)}_n\mathrm{pyz}]^{2+}$ and $[\mathrm{pyz(xyl)pyz}]^{2+}$ and the Ligand Dissociation of $[\mathrm{pyz(CH_2)}_n\mathrm{pyz}]^{2+}$ and $[\mathrm{pyz(xyl)pyz}]^{2+}$ from $[\mathrm{Fe(CN)_5L}]^{-}$ in Aqueous Solution[a]

ligand L^{n+}	$10^{-4}\,k_\mathrm{f}$,[b] $\mathrm{M^{-1}\,s^{-1}}$	$\Delta H_\mathrm{f}^{\ddagger}$, kJ $\mathrm{mol^{-1}}$	$\Delta S_\mathrm{f}^{\ddagger}$, J $\mathrm{K^{-1}\,mol^{-1}}$	$10^3\,k_\mathrm{d}$,[b] $\mathrm{s^{-1}}$	$\Delta H_\mathrm{d}^{\ddagger}$, kJ $\mathrm{mol^{-1}}$	$\Delta S_\mathrm{d}^{\ddagger}$, J $\mathrm{K^{-1}\,mol^{-1}}$
pyz[c]	0.038	64.4 ± 2.1	21 ± 8	0.42	110 ± 2	59 ± 8
$\mathrm{NH_2pyz}$	0.0367 ± 0.013	66.1 ± 3.8	27 ± 10	1.56	103 ± 6	48 ± 17
$\mathrm{CH_3pyz}$[d]	0.0475 ± 0.025	66.9 ± 1.3	32 ± 4	0.77	115	44
$[\mathrm{1\text{-}CH_3pyz}]^{+}$ [c]	0.243[e] 0.338 ± 0.013[f]	70.2 ± 2.0	42 ± 6	0.28	115 ± 2	75 ± 8
$[\mathrm{1\text{-}CH_3\text{-}3\text{-}NH_2pyz}]^{+}$	0.391 ± 0.08	66.1 ± 1.7	46 ± 5	304	101 ± 1	84 ± 3
$[\mathrm{1,2\text{-}(CH_3)_2pyz}]^{+}$				0.612	110 ± 1	62 ± 3
$[\mathrm{1,3\text{-}(CH_3)_2pyz}]^{+}$				4750	97 ± 2	92 ± 5
$[\mathrm{pyz(CH_2)_3pyz}]^{2+}$	2.63 ± 0.10	66.9 ± 1.7	64 ± 5	0.417	111 ± 6	62 ± 18
$[\mathrm{3\text{-}NH_2pyz(CH_2)_33\text{-}NH_2pyz}]^{2+}$	3.23 ± 0.07	61.1 ± 0.8	46 ± 3	69.3	90 ± 2	55 ± 6
$[\mathrm{pyz(CH_2)_4pyz}]^{2+}$	3.23 ± 0.06	61.9 ± 0.4	49 ± 2	0.636	102 ± 1	36 ± 3
$[\mathrm{pyz(CH_2)_5pyz}]^{2+}$	1.74 ± 0.11	64.6 ± 1.3	56 ± 4	0.478	105 ± 1	44 ± 3
$[\mathrm{pyz(CH_2)_6pyz}]^{2+}$	1.71 ± 0.08	66.9 ± 1.7	60 ± 5	0.502	106 ± 2	47 ± 6
$[\mathrm{pyz(CH_2)_7pyz}]^{2+}$	1.48 ± 0.04	66.1 ± 0.9	57 ± 2	0.362	112 ± 1	63 ± 3
$[\mathrm{pyz(CH_2)_8pyz}]^{2+}$	1.05 ± 0.03	62.2 ± 2.5	41 ± 8	0.336	110 ± 1	56 ± 3
$[\mathrm{pyz(CH_2)_5pyr}]^{2+}$	0.870 ± 0.022	66.1 ± 0.5	52 ± 2	0.391	107 ± 1	49 ± 3
$[\mathrm{pyz(}o\mathrm{\text{-}xyl)pyz}]^{2+}$	2.48 ± 0.12	66.9 ± 0.8	63 ± 3	0.288	110 ± 2	59 ± 5
$[\mathrm{3\text{-}NH_2pyz(}o\mathrm{\text{-}xyl)3\text{-}NH_2pyz}]^{2+}$	2.67 ± 0.09	62.8 ± 2.1	50 ± 6	321	101 ± 3	84 ± 10
$[\mathrm{2\text{-}CH_3pyz(}o\mathrm{\text{-}xyl)3\text{-}CH_3pyz}]^{2+}$				0.426		
$[\mathrm{3\text{-}CH_3pyz(}o\mathrm{\text{-}xyl)3\text{-}CH_3pyz}]^{2+}$	2.90 ± 0.06	70.7 ± 2.5	77 ± 8	3700	95 ± 4	83 ± 13
$[\mathrm{pyz(}p\mathrm{\text{-}xyl)pyz}]^{2+}$	1.35 ± 0.05	64.0 ± 0.4	49 ± 3	2.31	112 ± 3	60 ± 8

[a] At pH 7, $I = 0.10$ M (NaCl). [b] At 25.0 °C. [c] Reference 4, $I = 0.50$ M ($\mathrm{LiClO_4}$). [d] Reference 24. [e] Reference 4, $I = 0.10$ M ($\mathrm{LiClO_4}$). [f] This work.

order excess of $[\mathrm{Fe(CN)_5OH_2}]^{3-}$ over the monomeric species containing the bridging ligand, which was generated in solution by adding a slight stoichiometric excess of $[\mathrm{Fe(CN)_5OH_2}]^{3-}$ to L^{2+}. The observed first-order rate constants exhibited a linear dependence on the concentration of $[\mathrm{Fe(CN)_5OH_2}]^{3-}$, and the second-order rate constants k_2 and the corresponding activation parameters are presented in Table VI.

Kinetics of Dissociation Reactions. The kinetics of the dissociation of the ligand L^{2+} from $[\mathrm{Fe(CN)_5L}]^{-}$ complexes (eq 9)were investigated in aqueous solution at an ionic strength of 0.10 M (NaCl), using 0.25 M dimethyl sulfoxide (DMSO) to trap the five-coordinate $[\mathrm{Fe(CN)_5}]^{3-}$ intermediate. The $[\mathrm{Fe(CN)_5(DMSO)}]^{3-}$ complex is colorless ($\lambda_{\max} = 352$ nm, $\epsilon = 210$ $\mathrm{M^{-1}\,cm^{-1}}$) and is stable with respect to loss of DMSO ($k_\mathrm{d} = 7.5 \times 10^{-5}\ \mathrm{s^{-1}}$).[25] For a limiting D mechanism, the dissociation rate constant is independent of the nature and concentration of the entering ligand at high concentrations. The values of k_d measured for the $[\mathrm{Fe(CN)_5(pyz(CH_2)_3pyz)}]^{-}$ complex, for example, were found to be similar using 0.25 M pyrazine ($4.17 \times 10^{-4}\ \mathrm{s^{-1}}$) and a range of 0.10–0.50 M DMSO ($(4.37 \pm 0.34) \times 10^{-4}\ \mathrm{s^{-1}}$) as the entering ligand. The rate constants k_d and the corresponding activation parameters are presented in Table II for R = bpy, Table III for R = bpe, and Table IV for pyz, 3-$\mathrm{NH_2}$pyz, and 3-$\mathrm{CH_3}$pyz.

---

(25) Toma, H. E.; Malin, J. M.; Giesbrecht, E. *Inorg. Chem.* **1973**, *12*, 2084.

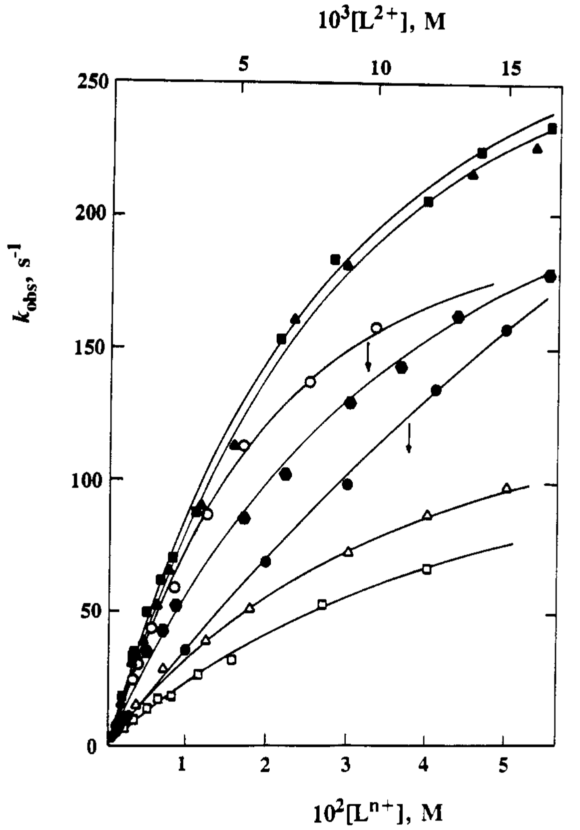

Figure 2. Plot of k_{obs} against $[L^{2+}]$ for the reaction of the $[Fe(CN)_5OH_2]^{3-}$ ion with ligands (■) $[3\text{-}NH_2pyz(CH_2)_33\text{-}NH_2pyz]^{2+}$, (▲) $[3\text{-}CH_3pyz(o\text{-}xyl)3\text{-}CH_3pyz]^{2+}$, (○) $[bpy(CH_2)_6bpy]^{2+}$, (●) $[pyz(o\text{-}xyl)pyz]^{2+}$, (●) $[1\text{-}CH_3\text{-}3\text{-}NH_2pyz]^+$, (△) $[pyz(p\text{-}xyl)pyz]^{2+}$, aand (□) $[bpy(o\text{-}xyl)bpy]^{2+}$ at 25.0 °C and $I = 0.10$ M (NaCl). The solid curves represent the fits of the data to eq 6 with the values of k_{-w} and K_{os} from Table V.

Table V. Outer-Sphere Ion-Pair Constants and Aqua Substitution Rates for the Reactions of $[Fe(CN)_5OH_2]^{3-}$ with L^{n+} ($I = 0.10$ M)

ligand L^{n+}	K_{os}, M^{-1}	k_{-w}, s^{-1}	ref
pyridine	≈1	300 ± 100	*a*
$[1\text{-}CH_3\text{-}3\text{-}NH_2pyz]^+$	20 ± 5	220 ± 70	*b*
$[bpy(CH_2)_6bpy]^{2+}$	50 ± 20	120 ± 50	*b*
$[bpy(o\text{-}xyl)bpy]^{2+}$	45 ± 5	95 ± 10	*b*
$[pyz(o\text{-}xyl)pyz]^{2+}$	95 ± 30	130 ± 20	*b*
$[pyz(p\text{-}xyl)pyz]^{2+}$	80 ± 10	90 ± 10	*b*
$[3\text{-}NH_2pyz(o\text{-}xyl)3\text{-}NH_2pyz]^{2+}$	50 ± 15	280 ± 60	*b*
$[3\text{-}NH_2pyz(CH_2)_33\text{-}NH_2pyz]^{2+}$	70 ± 10	230 ± 40	*b*
$[Co(NH_3)_5(4\text{-}CNpyr)]^{3+}$ [c]	597 ± 151	13.3 ± 2.4	*d*
$[Co(NH_3)_5(4\text{-}CNpyr)]^{3+}$ [e]	447 ± 21	20.1 ± 0.7	*d*
$[Co(NH_3)_5(3\text{-}CNpyr)]^{3+}$ [c]	799 ± 91	42.0 ± 3.1	*d*
$[Co(NH_3)_5(3\text{-}CNpyr)]^{3+}$ [e]	872 ± 40	26.5 ± 3.1	*d*
$[Co(NH_3)_5(DMSO)]^{3+}$	350 ± 80	20 ± 5	*f*
$[Co(NH_3)_5(im)]^{3+}$	670 ± 370	4.9 ± 1.6	*g*

[a] Reference 7. [b] This work. [c] Co–N(pyr). [d] Reference 14b. [e] Co–N(cyano). [f] Reference 11. [g] Reference 14a.

Table VI. Rate Constant and Activation Parameters for the Ligand Substitution Reactions of the $[Fe(CN)_5OH_2]^{3-}$ Ion with $[Fe(CN)_5L]^{(3-n)-}$ [a]

$[Fe(CN)_5L]^{(3-n)-}$	$10^{-3}\,k_2$,[b] M^{-1} s^{-1}	ΔH_2^*, kJ mol^{-1}	ΔS_2^*, J K^{-1} mol^{-1}	ref
$[Fe(CN)_5bpy]^{3-}$	0.050 ± 0.002			*c*
$[Fe(CN)_5(bpy(CH_2)bpy)]^-$	2.36 ± 0.24	67.8 ± 3.8	49 ± 11	*d*
$[Fe(CN)_5(bpy(CH_2)_2bpy)]^-$	1.70 ± 0.20			*d*
$[Fe(CN)_5(bpy(CH_2)_3bpy)]^-$	1.56 ± 0.15			*d*
$[Fe(CN)_5(bpy(CH_2)_4bpy)]^-$	1.32 ± 0.18			*d*
$[Fe(CN)_5(bpy(o\text{-}xyl)bpy)]^-$	1.61 ± 0.09	67.4 ± 1.7	42 ± 5	*d*
$[Fe(CN)_5pyz]^{3-}$	0.010 ± 0.001			*c*
$[Fe(CN)_5(pyz(CH_2)_6pyz)]^-$	1.45 ± 0.11			*d*
$[Fe(CN)_5(pyz(o\text{-}xyl)pyz)]^-$	1.45 ± 0.03	71.1 ± 3.8	54 ± 11	*d*

[a] At pH 7, $I = 0.10$ M (NaCl). [b] At 25.0 °C. [c] Reference 9. [d] This work.

$$[Fe(CN)_5L]^- + DMSO \xrightarrow{k_d} [Fe(CN)_5(DMSO)]^{3-} + L^{2+} \tag{9}$$

Discussion

The rate constants for the ligand substitution reactions of the $[Fe(CN)_5OH_2]^{3-}$ ion with the $[R(CH_2)_nR]^{2+}$, $[R(o\text{-}xyl)R]^{2+}$, and $[R(p\text{-}xyl)R]^{2+}$ dications are considerably larger than the values for the reactions with the neutral pyrazine, 4,4′-bipyridine, *trans*-1,2-bis(4-pyridyl)ethylene ligands, or their mono-N-methylated derivatives (Tables II–IV). These symmetrical dicationic ligands contain two potential coordination sites on the nitrogen donor atoms, a feature which should statistically increase their formation rate constants by a factor of 2, compared with ligands of the same charge but with only one donor atom. In the present study two asymmetric dicationic ligands bearing one donor atom, $[bpy(CH_2)_6PPh]^{2+}$ (Table II) and $[pyz(CH_2)_5py]^{2+}$ (Table IV), were prepared and their formation rate constants are approximately one-half the values for the corresponding symmetric ligands. In the case of the N-methylated tricationic ligand $[bpe(CH_2)_6bpeCH_3]^{3+}$, the increase in the charge on the ligand makes up for the loss of one of the potential coordination sites, resulting in little change in the value of k_f from that of the $[bpe(CH_2)_6bpe]^{2+}$ ligand (Table III). A slight dependence of ΔS^* on the charge of the entering ligand is also observed, with values in the ranges of 25–35 J K^{-1} mol^{-1} for L, 40–50 J K^{-1} mol^{-1} for L^+, and 30–80 J K^{-1} mol^{-1} for L^{2+}. This dependence has been observed previously for both the $[Fe(CN)_5OH_2]^{3-}$ [1,7] and $[Ru(CN)_5OH_2]^{3-}$ [26] aqua substitution reactions and is attributed to the entropy parameter, ΔS_{os}, associated with the outer-sphere association constants K_{os} ($\Delta H_{os} \approx 0$).[7] The enthalpies of activations fall in a relatively narrow range of values, 60–70 kJ mol^{-1} for $[Fe(CN)_5OH_2]^{3-}$, consistent with the dissociative loss of the coordinated aqua ligand.

For the dicationic ligands in this study, the observed first-order formation rate constants deviate from a linear dependence on $[L^{2+}]$ at high entering ligand concentration, indicating the onset of rate saturation. This behavior is consistent with an ion-pair dissociative substitution mechanism, involving a dissociative loss of the aqua ligand (k_{-w}) within an outer-sphere ion-pair complex (K_{os}) formed between $[Fe(CN)_5OH_2]^{3-}$ and L^{2+} (eqs 3–5). There are several methods for estimating the magnitude of K_{os} for the reactants in this study, each of which has its disadvantages. The values of ion-pair association constants are frequently calculated using the Eigen–Fuoss expression.[27] It is not very realistic to employ this model for the ligands in this study because of their nonspherical shape and the noncentric charge distributions. A calculation of K_{os} from the value of k_f ($=k_{obs}/[L^{2+}]$ at low concentrations of the entering ligand ($K_{os}[L^{2+}] \ll 1$, from eq 6) requires an assumption of the rate constant for aqua loss, which, from the study of the dications, appears to depend on the nature of the entering ligands. One possible problem with the determination of K_{os} from the fitting of k_{obs} to eq 6 is that, at the higher concentrations, the ionic strength, maintained at 0.10 M with added sodium chloride, is largely made up of contributions from the dicationic ligand itself. The values of K_{os} obtained by this method (Table V) are of a reasonable magnitude (20 M^{-1} for L^+ and 40–100 M^{-1} for L^{2+}) when compared to the ion-pair constants for the dications with $[Fe(CN)_6]^{4-}$ determined by visible spectrophotometric titrations (10–13 M^{-1} for L^+ and 150–200 M^{-1} for L^{2+}).

The aqua ligand dissociation rate constants calculated from the kinetics with the dicationic ligands are found in the range 90–130 s^{-1}, with the exceptions of the 3-amino-substituted

---

(26) Hoddenbagh, J. M. A.; Macartney, D. H. *Inorg. Chem.* **1986**, *20*, 380.

(27) (a) Eigen, M. *Z. Phys. Chem.* (*Frankfurt*) **1954**, *1*, 176. (b) Fuoss, R. M. *J. Am. Chem. Soc.* **1958**, *80*, 5059.

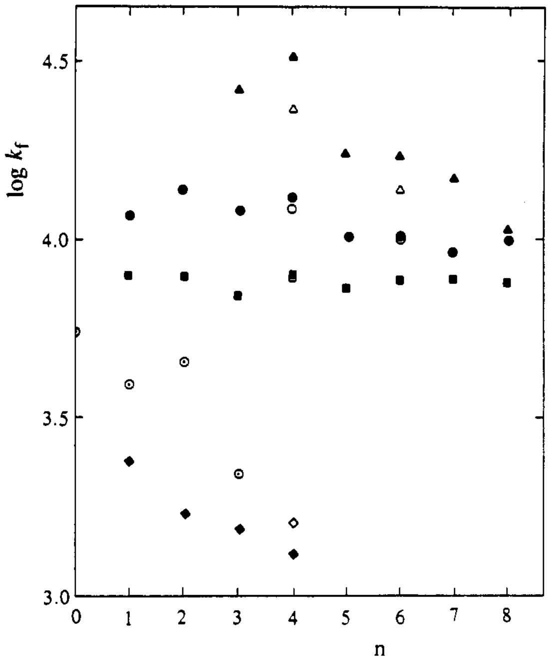

Figure 3. Plots of log k_f against the chain length n for the reactions of the $[Fe(CN)_5OH_2]^{3-}$ ion with (▲) $[pyz(CH_2)_npyz]^{2+}$, (●) $[bpy(CH_2)_nbpy]^{2+}$, (◆) $[(NC)_5Fe(bpy(CH_2)_nbpy)]^-$, and (■) $[bpe(CH_2)_nbpe]^{2+}$ (empty symbols for corresponding $[R(o\text{-xyl})R]^{2+}$ ($n = 4$) and $[R(p\text{-xyl})R]^{2+}$ ($n = 6$) ligands) at 25.0 °C and $I = 0.10$ M (NaCl) and (⊙) $[Co(NH_3)_5(bpy(CH_2)_nbpy)]^{3+}$ at 25.0 °C and $I = 0.10$ M ($LiClO_4$) from ref 13.

pyrazinium ligands, for which $k_{-w} = 230\text{–}280\ s^{-1}$. The higher values for the latter ligands may result from the presence of the two amino groups, which are potential donor groups and would increase the effective value of m in eq 6 to 4. Any coordination of the iron to an amino-N atom would likely be followed by rapid isomerization to the more stable pyrazine-N complex. Saturation kinetics have also been observed for the reactions of the $[Fe(CN)_5OH_2]^{3-}$ ion with a series of $[Co(NH_3)_5L]^{3+}$ species (L = 3- and 4-cyanopyridine, imidazole, DMSO)[11,14] as entering ligands, with k_{-w} and K_{os} falling in the ranges 5–42 s^{-1} and 350–870 M^{-1}, respectively. The reduced water dissociation rate constants, compared with 300 ± 100 s^{-1} estimated for neutral ligands such as pyridine, is likely a result of a more inert $Fe\text{–}OH_2$ bond within an ion-pair complex. A cationic ligand in the vicinity of the coordinated cyanides would tend to pull electron density away from the iron center and strengthen its interaction with the aqua ligand, in a manner similar to the decreased lability of the aqua ion upon protonation of a cyanide ligand on the $[Fe(CN)_5OH_2]^{3-}$ ion.[9,28] It appears from the data in Table V that the greater the stability of the ion pair, the lower the aqua dissociation rate constant.

For the aqua substitution reactions of the $[Fe(CN)_5OH_2]^{3-}$ ion, it has been observed that in addition to the total charge on the ligand, the positions of the charge(s) with respect to the donor atom(s) have a significant effect on the complexation rate constant. The rate constants for the reactions of the $[Fe(CN)_5OH_2]^{3-}$ ion with the series of $[R(CH_2)_nR]^{2+}$ ligands exhibit differing dependences on the length of the alkyl bridge, as depicted in the plot in Figure 3 of log(k_f) against n, the number of methylene groups in the bridge. The effect of n on the value of k_f is greatest for R = pyrazine, smaller for bipyridine, and negligible for *trans*-1,2-bis(4-pyridyl)ethylene. This follows a trend in the distance between the nitrogen donor atom and the site of the positive charge on each end of the ligand. The largest values of k_f are observed for the $[pyz(CH_2)_3pyz]^{2+}$, $[pyz(CH_2)_4pyz]^{2+}$, and $[pyz(o\text{-xyl})pyz]^{2+}$ ligands and substituted analogs. A strong "chelate" ion-pair formed between these dicationic ligands and the cyanide ligands on the $[Fe(CN)_5OH_2]^{3-}$ ion would place the N donor atoms in close proximity to the leaving aqua ligand. By the increasing of the lengths of either the N-heterocyclic end group and/or the polymethylene chain, the donor atoms are further removed from the site of substitution and a decrease in the second-order rate constant is observed. The same trend has been observed (Figure 3) in the rate constants for the entering ligands $[Co(NH_3)_5(py(CH_2)_npy)]^{3+}$ (n = 0–3).[13]

At sufficiently long chain lengths the rate constants for formation reactions with the three $[R(CH_2)_nR]^{2+}$ ligands tend to approach a limiting value, approximately twice that of the corresponding $[RCH_3]^+$ ligand, at about $6 \times 10^3\ M^{-1}\ s^{-1}$. It also appears, from the plots in Figure 3, that complexes containing even numbers of methylene groups in the chain generally form more rapidly than the corresponding odd-numbered value of n with one fewer methylene group. This may be due to the fluctuations in the relative distances between the positive charges on the ligand as the polymethylene chain conformation changes in solution with the value of n. With the o-xylyl- and p-xylyl-bridged ligands, which may be considered as four and six carbon bridges, respectively, the formation rate constants are somewhat smaller than for the corresponding $[R(CH_2)_4R]^{2+}$ and $[R(CH_2)_6R]^{2+}$ reactions (Figure 3). The differences in rate constants between the two types of ligands follows a trend in R, with pyz > bpy > bpe.

The rate constants for the formation of the bridged 2:1 complex, $[(NC)_5Fe(\mu\text{-}R(CH_2)_nR)Fe(CN)_5]^{4-}$, from the 1:1 species also exhibit a dependence on the length of the polymethylene chain (Table VI; Figure 3). While the entering ligand $[(CN)_5Fe(R(CH_2)_nR)]^-$ bears an overall charge of −1, the values observed for k_2 (and ΔS_2^*) are in the range between those reported for neutral and monocationic ligands. This phenomenon, observed with other entering ligands containing $[Fe(CN)_5]^{3-}$ centers, such as *trans*-$[Fe(CN)_5(\mu\text{-pyz})Ru(NH_3)_4(pyz)]^-$ ($k = 1.69 \times 10^3\ M^{-1}\ s^{-1}$)[29] and $[(Fe(CN)_5)_nRu(bpz)_3]^{(2-3n)+}$ ($k = 1.2 \times 10^4\ M^{-1}\ s^{-1}$ for n = 1, bpz = 2,2′-bipyrazine),[8] results from the relative proximities of the cationic and anionic centers to the donor atoms.

The rate constants and activation parameters measured for the dissociation of $[R(CH_2)_nR]^{2+}$ from $[Fe(CN)_5(R(CH_2)_nR)]^-$ in the presence of DMSO exhibit no appreciable trends with the length of the polymethylene chain, with the values of k_d falling in narrow ranges similar to the values for the corresponding $[RCH_3]^+$ ligands. The $[pyz(CH_2)_npyz]^{2+}$ ligands are the most inert toward substitution (with largest ΔH^* values) due to greater π-back-bonding from the iron(II) center than found with the bpy or bpe analogs. The presence of a methyl or amino substituent on the ring carbon adjacent to the N-donor atom greatly increases the rate of dissociation of the coordinated ligand on $[Fe(CN)_5L]^{(3-n)-}$ (Table IV). In addition to the increase in k_d, a decrease in ΔH^*, a measure of the Fe–N bond strength, is observed for the dissociation of the sterically strained ligand, compared with the unsubstituted analogs. The effects of steric hinderence on the metal–ligand bond strength has been observed previously for several $[Fe(CN)_5L]^{(3-n)-}$ complexes containing N- and S-donor ligands. Similar increases in the value of k_d for aminopyrazine compared with pyrazine (Table IV) have also been observed for quinoxaline ($k_d = 0.62 \pm 0.10\ s^{-1}$, $\Delta H^* = 82.0 \pm 8\ kJ\ mol^{-1}$, $\Delta S^* = 17 \pm 25\ J\ K^{-1}\ mol^{-1}$)[30] and N¹-bound 2-$CH_3$pyz ($k_d = 0.8\ s^{-1}$).[24] Other examples of steric strain on the Fe–L bond include penicillamine ($k_d = 1.34\ s^{-1}$) compared with cysteine (0.104 s^{-1}),[6] 2-cyanopyridine (1.19 s^{-1}) compared with pyridine ($1.10 \times 10^{-3}\ s^{-1}$),[31] N³-bound histidine (0.109 s^{-1}) compared with N¹-bound histidine ($5.3 \times 10^{-4}\ s^{-1}$),[5] and $[Co(NH_3)_5(3\text{-}CH_3pyz)]^{3+}$ (11 s^{-1}) compared with $[Co(NH_3)_5pyz]^{3+}$ ($\approx 3 \times 10^{-4}\ s^{-1}$).[12]

---

(28) Malin, J. M.; Koch, R. C. *Inorg. Chem.* **1978**, *17*, 752.

(29) Toma, H. E. *J. Coord. Chem.* **1978**, *7*, 231.

(30) Coelho, A. L.; Toma, H. E.; Malin, J. M. *Inorg. Chem.* **1983**, *22*, 2703.

(31) Szecsy, A. P.; Miller, S. S.; Haim, A. *Inorg. Chim. Acta* **1978**, *28*, 189.

The more rapid rates of ligands dissociation observed for the complexes containing the 3-methyl-1-alkylpyrazinium ligands, compared to the 3-amino counterparts, are due to a combination of steric and electronic effects. The methyl group extends further from the pyrazinium ring than the amino group and also has a slightly larger van der Waals radius. This results in a greater steric strain on the Fe–N bond in the methyl-substituted ligands. The steric strain energy, ΔG_{strain}, may be calculated using eq 10,

$$\Delta G_{\text{strain}} = -RT \ln(k_{\text{d}}/k_{\text{d}'}) \qquad (10)$$

where k_{d} and $k_{\text{d}'}$ are the ligand dissociation rate constants for the sterically hindered ligand and the nonhindered analog, respectively.[30] For the pyrazinium ligands in this study (Table IV), the steric strain energies are 17 ± 1 and 22 ± 1 kJ mol^{-1} for the 3-amino- and 3-methyl-substituted ligands, respectively. Strain energies of 13–14 kJ mol^{-1} have been reported for sterically hindered 4,5-dimethylimidazole[32] and N^3-bound histidine[5] ligands.

The MLCT transition energies for the (3-methylpyrazinium)- and the (3-amino-pyrazinium)pentacyanoferrate(II) complexes indicate that the π-back-bonding in the amino complexes is less than in the methyl analogs, reducing the Fe–N bond strength. With the dissociation rate constants of the methyl-substituted ligands generally 10–15 times larger than amino-substituted derivatives, it is clear that the steric effects greatly outweigh the electronic effects in these reactions. In the case of the dissociation of the $[(NC)_5Fe(\mu\text{-}3\text{-}Xpyz)Fe(CN)_5]^{6-}$ complexes, the rate constants for X = NH_2 and CH_3 are very rapid (compared with $[(NC)_5Fe(\mu\text{-}pyz)Fe(CN)_5]^{6-}$ at $\approx 1 \times 10^{-4}$ s^{-1}) and are quite similar to each other (Table IV). With both the iron(II) centers at the nonsterically hindered N atom and the amine or methyl substituents donating electron density to the pyrazine ring, there is likely little π-back-bonding from the iron(II) at the sterically hindered N atom. Both steric and electronic effects, therefore, are responsible for the very labile Fe–N bond in these bridged complexes.

The $[bpy(CH_2)_nbpy]^{2+}$ ligands with longer alkane bridges, $n = 8\text{–}12$, have been observed to form strong inclusion complexes with α-cyclodextrin (α-CD), a cyclic oligosaccharide host molecule.[33,34] In these guest–host complexes the 4,4′-bipyridinium groups extend out from either end of the cyclodextrin cavity, with the alkane bridge residing in the hydrophobic interior. A kinetic study on the reaction of $[bpy(CH_2)_{10}bpy]^{2+}$ with the $[Fe(CN)_5OH_2]^{3-}$ ion indicates that inclusion of the entering ligand within the α-CD cavity significantly decreases the formation rate constant from $(7.3 \pm 0.2) \times 10^3$ to $(3.0 \pm 0.2) \times 10^3$ M^{-1} s^{-1}. Complexation of the α-CD-threaded $[bpy(CH_2)_nbpy]^{2+}$ ligand by $[Fe(CN)_5OH_2]^{3-}$ ions at both free nitrogens results in the formation of novel metal rotaxane complexes of the type $[(NC)_5Fe\{bpy(CH_2)_nbpy\cdot\alpha\text{-}CD\}Fe(CN)_5]^{4-}$.[33] The preparation of similar rotaxanes complexes using other symmetric and asymmetric ligands such as $[pyz(CH_2)_npyz]^{2+}$ and $[pyz(CH_2)_nbpy]^{2+}$ ligands is underway in our laboratory.

Acknowledgment. The authors acknowledge the Natural Sciences and Engineering Research Council of Canada for financial support, in the form of operating and equipment grants (D.H.M.) and an Undergraduate Student Research Award (L.J.W.). We thank Queen's University for a research grant from its Advisory Research Committee and a graduate scholarship (D.A.F.). C. A. Waddling and R. S. Wylie are thanked for experimental assistance and helpful discussions.

---

(32) Shepherd, R. E. *J. Am. Chem. Soc.* **1976**, *93*, 3329.

(33) Wylie, R. S.; Macartney, D. H. *J. Am. Chem. Soc.* **1992**, *114*, 3136.

(34) Wylie, R. S.; Macartney, D. H. *Supramol. Chem.*, in press.